3D Tooth Loss Detection and Dataset from Intraoral Scans for Automation in Dental Implant Placement

Soomin Ham[1], Junsu Kim[2], Deok-Yeong Kim[3], Ji-Man Park[3], Kyungdon Joo[2]
[1]DI Robotics Inc., Seoul, South Korea
[2]Graduate School of Artificial Intelligence, UNIST, Ulsan, South Korea
[3]Department of Prosthodontics & Dental Research Institute, Seoul National University School of Dentistry, Seoul, South Korea

***Abstract*—We present an AI-driven framework for the 3D detection of edentulous areas and the estimation of appropriate positions and orientations for dental implant placement based on 3D dental scans. To address the challenge of data scarcity for training, we have generated a new dataset named 3D Tooth Loss (3D-TL) using publicly available intraoral 3D scans. Our framework integrates a pre-trained instance segmentation model with a Point transformer-based 3D bounding box refinement model to enhance detection accuracy. Quantitative and qualitative evaluations show significant improvements in 3D detection performance, positioning estimation, and clinical validation, confirming our framework's effectiveness in automating dental implant planning and placement.**

***Keywords*—tooth loss, missing teeth, intraoral scans, dental implant placement, implant planning, digital dentistry, dental model, 3D mesh, 3D point clouds, 3D detection, deep learning**

I. INTRODUCTION

Recent advances in artificial intelligence (AI) are significantly enhancing surgical techniques and dental procedures in both preclinical and clinical studies [1]. AI shows growing potential in various dental applications [2, 3], including diagnosis, patient care, and most notably, in surgical planning and simulation.

To automate the dental implant surgery process, we deploy AI solutions to detect edentulous areas and estimate appropriate dental implant placement positions, thus streamlining the procedure and enhancing both efficiency and accuracy. However, the inherent diversity in tooth structures and the variations among individuals (e.g. number, size, and location of teeth) are considerable; therefore, they pose challenges and should be carefully considered.

Automating dental implant placement requires accurately identifying toothless areas and determining the positions and orientations of implants in three dimensions (3D). While the recognition of existing teeth using neural networks in 2D has been extensively studied [4, 14, 15, 16], research on estimating the 3D locations of missing teeth for implant placement remains limited. This task is distinct from recognizing semantic information such as segmenting existing teeth, because it involves predicting the features of non-existent objects, making pre-trained or *off-the-shelf* networks less effective. Additionally, acquiring sufficient clinical data on patients with one or more missing teeth to train deep neural networks presents a significant challenge.

To address the scarcity of training data on missing teeth for 3D dental implant applications, we introduce a new 3D Tooth Loss (**3D-TL**) dataset derived from 3D intraoral scans. We also propose a framework for detecting edentulous areas and estimating implant placement parameters in 3D. Our 3D tooth loss detection approach involves three stages and we validate the effectiveness of our framework and dataset through evalu-

E-mail: [1]smham21@gmail.com, [2]{junsu0109, kyungdon}@unist.ac.kr, [3]{thekyeong, jimarn}@snu.ac.kr

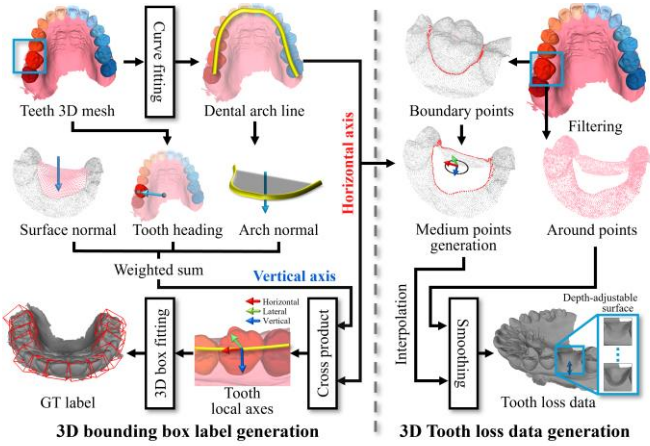

Fig. 1. 3D Tooth Loss (3D-TL) Dataset Generation. To train the model, we generate tooth loss point cloud data from the public dataset [5] and construct 3D bounding box labels for tooth loss detection.

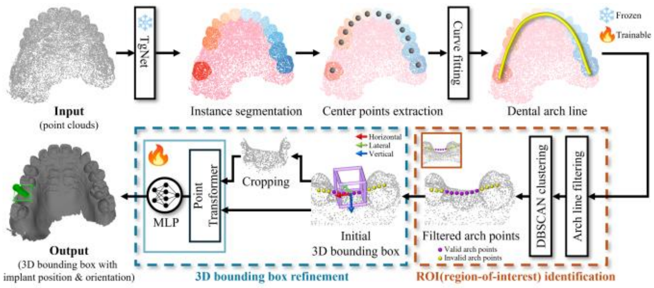

Fig. 2. 3D Tooth Loss Detection. Our framework begins by utilizing TgNet [6] trained on the Teeth3DS [5] dataset, to segment each instance, extract the dental arch line, and identify the ROI for the missing tooth. The initial 3D bounding box is then refined using a Point transformer-based [7] 3D bounding box refinement model.

ation metrics. Furthermore, by aligning pre-dictions from intraoral scans (i.e. surface scans) with corresponding CBCT scans, we confirm their practical viability and potential for clinical translation.

II. METHODS

A. 3D Tooth Loss (3D-TL) Dataset Generation

To generate training data for a 3D tooth loss detection framework, we preprocess 3D meshes of intraoral scans from the public clinical dataset Teeth3DS [5] and utilize the provided ground truth instance labels. Initially, we extract point clouds from the 3D mesh vertices and randomly select a label that follows the FDI dental notation system for the tooth to be removed, resulting in 3D point cloud data with one tooth missing. Using a KDTree [8], we identify points at the gingival margin (i.e. the boundary points). To adjust the depth of the gingival surface, we generate medium points and modify them along the surface normal vector (right in Fig. 1).

To determine the surface normal for the toothless area, we first use B-spline curve fitting [9] on the centroids of tooth instances to extract a dental arch line (see Fig. 1 left). The Teeth3DS [5] dataset provides ground truth labels for each tooth instance. From the centroid of the tooth to be removed, we identify the two closest points among 100 sampled points on the arch line to establish a *horizontal axis*. Next, we search for pairs of boundary points perpendicular to the horizontal axis, apply linear interpolation to these pairs, and then use PCA [10] to compute the *surface normal*. Circular medium points are generated based on the specified surface (hollow) depth and the computed surface normal. These medium points are combined with the boundary points and linearly interpolated to generate initial surface points (see Fig. 1 right). Finally, the initial surface points, along with the around points, are smoothed using a moving average filter applied only in the vertical direction to produce depth-adjustable, surface-completed point clouds.

To construct the 3D bounding box label for tooth loss data, we first establish a horizontal axis and a surface normal, as previously determined. Next, we compute an *arch normal* using PCA on 100 sampled points from the dental arch (see Fig. 1 left). Utilizing the gingival point clouds from the Teeth3DS ground truth labels, we establish a *tooth heading vector* from the centroid of these gingival points towards the tooth loss region (i.e. the missing tooth). By combining the surface normal, arch normal, and tooth heading vector with different weight scales, we establish the *vertical axis* of the missing tooth. The cross-product of the horizontal and vertical axes yields an orthogonal lateral axis for the missing tooth. Using these three axes, we measure the closest and farthest distances from the centroid along each axis to determine the 3D bounding box dimensions that fit the missing tooth region (left in Fig. 1). Through this process, we generate the **3D-TL** dataset, consisting of 4,200 training, 1,152 validation, and 888 test dental scan models. Each set includes 3D point clouds and 3D bounding box labels, all featuring tooth loss for implant placement.

B. 3D Tooth Loss Detection Framework

First, we input the 3D-TL data into the instance segmentation model, TgNet [6], which is trained with the Teeth3DS [5] dataset. This model demonstrated the highest performance in the 3DTeethSeg'22 challenge [6], allowing us to obtain instance segmentation labels for each tooth (Fig. 2).

Next, we estimate the initial 3D bounding box via region-of-interest (ROI) identification. Using the centroid of each tooth obtained from the instance segmentation results, we extract an arch line through B-spline curve fitting and sample 100 points on the arch line. By searching the input point clouds closest to each sampled point in the vertical direction, we filter the sampled points on the arch line that correspond to the missing tooth region. Subsequently, we apply DBSCAN [11] clustering to the filtered points to eliminate outliers, robustly identifying the *valid* filtered points within the missing tooth region (bottom in Fig. 2). We then calculate the mean of these valid points to determine the *initial 3D location*. We use PCA to determine an *arch normal* and establish a *tooth heading vector* from the center of gingival points towards the initial 3D location. By combining the arch normal and tooth heading vector with different weight scales, we establish an initial *vertical axis*.

Lastly, to refine the initial 3D bounding box, we configure a 3D bounding box refinement model employing the Point transformer [7] as the backbone and multi-layer perceptron (MLP) [12] layers for the header network (see Fig. 2 bottom). The Point transformer is initialized with pre-trained instance segmentation weights, while the MLP header is randomly initialized. As input, we crop the tooth point clouds around the initial 3D bounding box to facilitate feature extraction. During model training, the location and dimensions are regressed using the L1 loss function, the rotation is regressed using a weighted L2 loss function, and a cosine distance loss defined as 1-cosine similarity is applied to the *vertical axis* which serves as the principal axis for implant positioning.

TABLE I. 3D BOUNDING BOX EVALUATION ON 3D-TL TEST DATA MEAN ± STD

Metric \ Method	Initial 3D bounding box	3D Tooth Loss Detection (trained from the scratch)	3D Tooth Loss Detection
3D IoU ↑	0.468 ± 0.169	0.652 ± 0.208	**0.724** ± **0.200**
$\mathbf{E_d}$ ↓ [mm]	3.446 ± 7.967	2.478 ± 7.164	**1.585** ± **5.048**
$\mathbf{C_S}$ (horizontal) ↑	0.939 ± 0.275	0.989 ± 0.042	**0.993** ± **0.024**
$\mathbf{C_S}$ (vertical) ↑	0.923 ± 0.296	0.957 ± 0.180	**0.966** ± **0.175**
$\mathbf{C_S}$ (lateral) ↑	0.937 ± 0.230	0.958 ± 0.177	**0.966** ± **0.173**

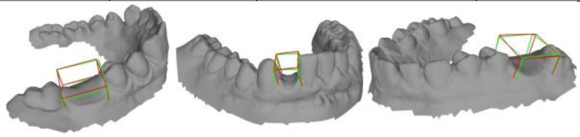

Fig. 3. Qualitative results on 3D-TL test data. Ground truth 3D bounding box labels (red boxes) and predicted labels (green boxes) are shown.

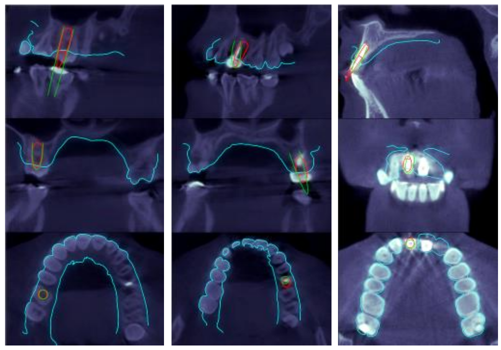

Fig. 4. Qualitative results from clinical test data. Visualization of implant positions in the missing tooth regions: #16 (left), #25 (middle), and #11 (right). Intraoral scans (3D mesh) are aligned with the corresponding CBCT scans and cross-sectional images are shown. Cyan lines indicate the intraoral scan within each CBCT plane; red lines represent the expert's implant ground truth; green lines are the estimated implant positions.

III. EXPERIMENTS AND RESULTS

We use PyTorch and an NVIDIA RTX A5000 to train the 3D bounding box refinement model, which requires about 4GB of memory with a batch size of 8 for 100 epochs (~6 hours). Using the SGD optimizer, we schedule the learning rate via cosine annealing, ranging from 1e-2 to 1e-6. We sample 20K point clouds from 3D-TL data as input to infer instance segmentation results and use cropped data with 2K point clouds to train the 3D bounding box refinement. To regress the 3D bounding box, we predict ten parameters: location, rotation in quaternions, and dimensions. Our evaluation metrics include the 3D Intersection over Union [13] (3D IoU) between the predicted and ground truth 3D bounding boxes, the Euclidean distance ($\mathbf{E_d}$) error for the box center in 3D, and the cosine similarity ($\mathbf{C_s}$) of each of the three axes for oriented 3D bounding boxes. We evaluate and validate our 3D tooth loss detection framework using both quantitative (see Table I) and qualitative results (Fig. 3 and 4). Our refinement model and the 3D-TL dataset demonstrate improved accuracy across comprehensive evaluation metrics, with clinical validation on test data suggesting practical feasibility.

IV. Discussion and Conclusion

Integrating AI into dental procedures, particularly through our 3D tooth loss detection framework, improves the accuracy and efficiency of implant planning and placement. We have also generated a new 3D Tooth Loss (**3D-TL**) dataset using intraoral 3D scans, effectively addressing the challenge of limited data availability for training AI models. Our framework automates the identification of edentulous areas and estimates appropriate positions for implant placement, which we validate through metric-based evaluation and alignment of predictions with CBCT scans. While positioning for implants typically relies on CT data, our study exclusively utilizes surface information from 3D intraoral scans. Despite the inherent limitations of using only surface data, our method shows both quantitative and qualitative feasibility in estimating implant positions. This suggests that further optimizations, along with the integration of anatomical information from CT scans, could refine the results. These refinements would improve both the accuracy and reliability of our approach in future clinical (*in vivo*) studies. This advancement represents a significant step forward in automation, streamlining workflows and enhancing the efficiency of dental implant procedures.

References

[1] Fatima, Anum, et al. "Advancements in dentistry with artificial intelligence: current clinical applications and future perspectives." *Healthcare*. Vol. 10. No. 11. MDPI, 2022.

[2] Shan, T., F. R. Tay, and L. Gu. "Application of artificial intelligence in dentistry." *Journal of dental research* 100.3 (2021): 232-244.

[3] Carrillo‐Perez, Francisco, et al. "Applications of artificial intelligence in dentistry: A comprehensive review." *Journal of Esthetic and Restorative Dentistry* 34.1 (2022): 259-280.

[4] Tuzoff, Dmitry V., et al. "Tooth detection and numbering in panoramic radiographs using convolutional neural networks." *Dentomaxillofacial Radiology* 48.4 (2019): 20180051. R. Nicole, "Title of paper with only first word capitalized," J. Name Stand. Abbrev., in press.

[5] Ben-Hamadou, Achraf, et al. "Teeth3ds: a benchmark for teeth segmentation and labeling from intra-oral 3d scans." *arXiv preprint arXiv:2210.06094* (2022).

[6] Ben-Hamadou, Achraf, et al. "3DTeethSeg'22: 3D Teeth Scan Segmentation and Labeling Challenge." *arXiv preprint arXiv:2305.18277* (2023).

[7] Zhao, Hengshuang, et al. "Point transformer." *Proceedings of the IEEE/CVF international conference on computer vision*. 2021.

[8] Bentley, Jon Louis. "Multidimensional binary search trees used for associative searching." *Communications of the ACM* 18.9 (1975): 509-517.

[9] Park, Hyungjun, and Joo-Haeng Lee. "B-spline curve fitting based on adaptive curve refinement using dominant points." *Computer-Aided Design* 39.6 (2007): 439-451.

[10] Minka, Thomas. "Automatic choice of dimensionality for PCA." *Advances in neural information processing systems* 13 (2000).

[11] Ester, Martin, et al. "A density-based algorithm for discovering clusters in large spatial databases with noise." *kdd*. Vol. 96. No. 34. 1996.

[12] Gardner, Matt W., and S. R. Dorling. "Artificial neural networks (the multilayer perceptron)—a review of applications in the atmospheric sciences." *Atmospheric environment* 32.14-15 (1998): 2627-2636.

[13] Ahmadyan, Adel, et al. "Objectron: A large scale dataset of object-centric videos in the wild with pose annotations." *Proceedings of the IEEE/CVF conference on computer vision and pattern recognition*. 2021.

[14] Kılıc, Münevver Coruh, et al. "Artificial intelligence system for automatic deciduous tooth detection and numbering in panoramic radiographs." *Dentomaxillofacial Radiology* 50.6 (2021): 20200172

[15] Jader, Gil, et al. "Deep instance segmentation of teeth in panoramic X-ray images." *2018 31st SIBGRAPI Conference on Graphics, Patterns and Images (SIBGRAPI)*. IEEE, 2018.

[16] Lee, Jae-Hong, et al. "Detection and diagnosis of dental caries using a deep learning-based convolutional neural network algorithm." *Journal of dentistry* 77 (2018): 106-111.